

## NMR spectra from Monte Carlo simulations of polymer dispersed liquid crystals

C. Chiccoli,<sup>1</sup> P. Pasini,<sup>1</sup> G. Skačej,<sup>2</sup> C. Zannoni,<sup>3</sup> and S. Žumer<sup>2</sup>

<sup>1</sup>*Istituto Nazionale di Fisica Nucleare, Sezione di Bologna, Via Irnerio 46, I-40126 Bologna, Italy*

<sup>2</sup>*Physics Department, University of Ljubljana, Jadranska 19, SI-1000 Ljubljana, Slovenia*

<sup>3</sup>*Dipartimento di Chimica Fisica ed Inorganica, Università di Bologna, Viale Risorgimento 4, I-40136 Bologna, Italy*

(Received 30 March 1999)

We present the calculation of NMR line shapes, including dynamical effects, of polymer dispersed liquid crystals starting from the Monte Carlo configurations simulated for a lattice spin model. We consider droplets with radial, bipolar, and random boundary conditions and examine to what extent their predicted deuterium NMR spectra differ in the presence of molecular motion. [S1063-651X(99)09910-9]

PACS number(s): 61.30.Cz, 61.30.Gd

### I. INTRODUCTION

Polymer dispersed liquid crystals (PDLC) [1] are materials that consist of microscopic nematic droplets, with typical radii from a few hundred Ångström to well above a micron, embedded in a polymer matrix. These systems are interesting both for technical applications and for an understanding of the behavior of mesophases in a confined environment. PDLC droplets also represent practical realizations of systems exhibiting topological defects of interest in many fields of physics [1]. Various experimental works like calorimetry, polarized light experiments, and NMR investigations have considered these microconfined systems with different boundary conditions at the droplet surface. In particular, radial [2,3] or axial structures [3] for homeotropic surface anchoring and toroidal [4] or bipolar [2,3,5] structures for tangential anchoring are commonly found, depending on the polymer matrix chosen and on the preparation methods. Additional effects of interest come from the application of an external electric or magnetic field [2]. From the theoretical point of view, Landau–de Gennes elastic continuum approaches [1] and Monte Carlo (MC) simulations [6] have been used to study PDLC in a variety of these physical situations. In particular, the MC technique has proved to be a powerful method not only for investigating the thermodynamical behavior of confined nematics, but also for simulating quantities that can be observed directly in real experiments. Methodologies needed to calculate powder deuterium NMR line shapes and textures observable in polarized light experiments corresponding to the microscopic configurations found have been developed [6]. Here we wish to present a more widely applicable methodology that aims to reproduce <sup>2</sup>H NMR spectra starting from MC configurations, taking into account also dynamical effects such as fluctuations of molecular long axes and translational molecular diffusion. In the next section we recall briefly the model used in our simulation, in Sec. III we describe the method proposed to calculate the line shape, while in Sec. IV we show and discuss the results.

### II. MONTE CARLO SIMULATIONS

The computer simulations considered here are based on a simple model system put forward by Lebwohl and Lasher

(LL) many years ago [7] to mimic the nematic behavior of a nematic liquid crystal. It reproduces a weak first order transition for a bulk, i.e., for a large sample with periodic boundary conditions [7,8], while in a confined system with radial or tangential boundary conditions of sufficiently small size the phase transition is suppressed [9] in agreement with experiments. The LL model is a lattice of “spins” where each “spin” can represent either one uniaxial molecule or a closely packed cluster of molecules which maintains its short range order in the relatively narrow temperature range of existence of the nematic as well as across the disordering phase transition [6]. The  $N$  particles (spins) of the model system interact through a pair potential of the form

$$U_{ij} = -\epsilon_{ij} P_2(\cos \beta_{ij}) = -\epsilon_{ij} \left[ \frac{3}{2} (\mathbf{u}_i \cdot \mathbf{u}_j)^2 - \frac{1}{2} \right], \quad (1)$$

where  $\epsilon_{ij}$  is a positive constant for nearest neighbor spins  $i$  and  $j$  and zero otherwise,  $P_2$  is the second-rank Legendre polynomial, and  $\beta_{ij}$  is the angle between the three-dimensional unit vectors  $\mathbf{u}_i$  and  $\mathbf{u}_j$  located at the lattice sites.

To model a PDLC droplet a jagged sphere is carved from the cubic lattice by considering all the molecules lying closer than  $R$  (the droplet radius) to the chosen center. Further, the interaction with the polymer is mimicked by assuming an additional layer of spins whose orientations are chosen in accordance with the desired boundary conditions [10]. During the last few years, some of the present authors have studied PDLC droplets with different boundary conditions using Monte Carlo simulations [9–11].

In the present work we consider droplets with radial, bipolar, and random boundary conditions. We perform Monte Carlo (MC) simulations as follows. For radial and bipolar boundary conditions the calculations at the lowest temperature start from perfectly ordered (zero-temperature) configurations. These are, in accordance with the given boundary conditions, a perfect hedgehog and a perfect bipolar structure in the radial and bipolar cases, respectively. In case of random boundary conditions, however, the initial particle orientations inside the droplet are selected randomly. At higher temperatures the simulation starts from an already equilibrated configuration at the nearest lower temperature, when this is available. The Metropolis procedure [12] is then used to update the lattice for a certain number of cycles, i.e., of sets of  $N$  attempted moves. Each particle is selected at ran-

dom for a trial move at every lattice sweep using a random shuffling algorithm [8]. A new trial orientation of the chosen particle is then generated by a controlled variation from the previous one [13]. We have checked that a rejection ratio not too far from 0.5 is achieved while ensuring that an adequate evolution is obtained. For all types of boundary conditions the number of particles (spins) inside the droplet was set to 5832, whereas in the additional surface layer fixing the boundary conditions to 1352.

The numerical output from our Monte Carlo (MC) simulation consists of full sets of “spin coordinates” and their direction cosines. While these detailed data are very interesting to investigate the molecular organization inside droplets, it is not so easy to relate them to macroscopic observables. We have then decided to calculate, starting from these microscopic configurations, observables that can be measured in real experiments and cover, in such a way, the gap between theory and experiments. In previous papers [6,14] we have calculated  $^2\text{H}$  NMR spectra from MC configurations in the absence of motions. We have shown that these “powder” spectra differ for radial, bipolar, and toroidal boundary conditions in a way that could allow assigning the boundary condition type from an inspection of the NMR spectra. In real experiments the presence of diffusive motion resulting in the modulation of the quadrupolar interaction on the NMR time scale cannot be excluded and might smear out totally (or in part) the characteristic spectral features, making the boundary condition assignment more troublesome or altogether impossible. In the following section we re-examine the calculation of NMR spectra and discuss the inclusion of dynamics, while later on we shall discuss the spectral differences between various boundary conditions.

### III. NUCLEAR MAGNETIC RESONANCE

Deuterium nuclear magnetic resonance ( $^2\text{H}$  NMR) [2,15–17] is a powerful experimental technique that is most frequently applied to investigate polymer dispersed liquid crystals (PDLC). It is very convenient for the study of such heterogeneous systems since using deuterated nematics the resulting spectra only give direct information on the behavior of the liquid crystal confined to spherical cavities inside the nondeuterated polymer matrix. Further, it is applicable also for small, i.e., submicron droplets, where optical methods fail to yield useful information because the light wavelength is too large compared to the droplet diameter.  $^2\text{H}$  NMR spectra give an idea about the orientational molecular ordering inside nematic droplets, that is both about director configurations and dynamic processes such as molecular fluctuations and diffusion.

A  $^2\text{H}$  NMR spectrum of a selectively deuterated nematic in the bulk isotropic phase consists of a single line whose position in the spectrum is determined by the Zeeman splitting of deuteron energy levels in the spectrometer magnetic field and whose width is well below 100 Hz. Since deuterons possess a nonzero quadrupolar moment, there is an additional perturbative contribution to their energy levels coming from quadrupolar interactions between them and the electric field gradient (EFG) of the C—D bonds in nematic molecules. These anisotropic perturbative contributions are averaged out by molecular motions in the isotropic, but not in the

nematic phase. Indeed, once in an undistorted nematic phase, the single narrow line splits into a doublet, the frequency splitting now being typically of the order of  $\delta\nu_Q \sim 100$  kHz. In general, it depends on the relative orientation of the EFG tensor and the direction of the NMR spectrometer magnetic field  $\mathbf{B}$ . It is instructive to introduce motional averaging depending on the rate of the corresponding molecular motion. Molecular rotations (mainly around the long molecular axis) usually occur on a time scale faster than the scale related to the order fluctuations and molecular self-diffusion. Therefore, we assume that the effective EFG tensor averaged over molecular rotations is uniaxial, with the principal axis along the long molecular axis  $\mathbf{a}$ . The quadrupolar frequency splitting so depends only on the relative orientation of the unit vector  $\mathbf{a}$  and  $\mathbf{B}$ , and is given by  $\Omega_Q = \pm \delta\omega_Q \frac{1}{2} [3(\mathbf{a} \cdot \mathbf{B}/B)^2 - 1]$ , where  $\delta\omega_Q = 2\pi\delta\nu_Q$  represents the maximum effective splitting averaged over fast molecular rotations. In a nematic phase, however, the molecular long axes  $\mathbf{a}$  are not fixed and fluctuate around an average value, denoted by a unit vector  $\mathbf{n}$  called the director. An average over these fluctuations can be easily performed only if they are also rapid enough on the NMR time scale, which results in an additional reduction of the quadrupolar splitting. Neglecting biaxiality in molecular ordering, this effective splitting can be written as (see, for instance, Refs. [1,18,19])

$$\omega_Q = \pm \delta\omega_Q S \left[ \frac{3 \cos^2 \theta - 1}{2} \right], \quad (2)$$

where  $S$  is the usual uniaxial nematic order parameter defined by the ensemble average  $S = \langle \frac{1}{2} [3(\mathbf{n} \cdot \mathbf{a})^2 - 1] \rangle$ , and  $\theta$  is the angle between the local director  $\mathbf{n}$  and the magnetic field  $\mathbf{B}$ . Alternatively, the order parameter  $S$  can be calculated also as the largest eigenvalue of the ordering matrix [20].

In confined nematics, e.g., in PDLC, the director is position dependent,  $\mathbf{n} = \mathbf{n}(\mathbf{r})$  reflecting boundary conditions imposed by the polymer matrix. Moreover, in the vicinity of the confining substrates the value of the order parameter  $S$  describing the degree of molecular ordering may differ from its value in the bulk, which results in  $S = S(\mathbf{r})$ . Consequently, the corresponding contributions to the  $^2\text{H}$  NMR line splitting  $\omega_Q(\mathbf{r})$  depend on  $\mathbf{r}$  as well. Since the NMR spectrum corresponds to the overall response of all molecules present in the sample, each of the director configurations  $\mathbf{n}(\mathbf{r})$  appearing inside the droplet yields a specific contribution. The identification of these director configurations can, however, be very problematic since molecular self diffusion affects the  $^2\text{H}$  NMR line shape significantly. Only in the absence of significant molecular diffusion the spectra can be calculated simply as a superimposition of individual molecular static lines of Lorentzian shape from all over the sample, these lines being positioned into the spectrum according to  $\mathbf{n}(\mathbf{r})$  and  $S(\mathbf{r})$  used in Eq. (2) (see Ref. [14]).

In this paper we wish to extend the analysis to include also dynamic effects, such as fluctuations of molecular long axes  $\mathbf{a}$  (defining the order parameter  $S$  and the director  $\mathbf{n}$ ) and the translational molecular diffusion. For this purpose it is convenient to use a semiclassical approach with the time-

dependent spin Hamiltonian [19] where the  $^2\text{H}$  NMR line shape  $I(\omega)$  is calculated as the Fourier transform of the relaxation function  $G(t)$ ,

$$I(\omega) = \int \exp(i\omega t) G(t) dt, \quad (3)$$

where  $G(t)$  is generated as

$$G(t) = \exp(i\omega_Z t) \left\langle \exp\left( i \int_0^t \Omega_Q[\mathbf{r}_i(t'), t'] dt' \right) \right\rangle_i, \quad (4)$$

with  $\Omega_Q[\mathbf{r}_i(t), t] = \pm \delta\omega_Q \frac{1}{2} [3(\mathbf{a}_i \cdot \mathbf{B}/B)^2 - 1]$ , the ‘‘instantaneous’’ quadrupolar splitting [not to be confused with  $\omega_Q$  from Eq. (2), where an average over fluctuations of  $\mathbf{a}_i$  has already been performed]. Further, in Eq. (4)  $\omega_Z$  denotes the Zeeman frequency, while the brackets  $\langle \dots \rangle_i$  stand for the ensemble average over all molecules in the sample. The resonance frequency of the  $i$ th molecule located at  $\mathbf{r}_i$  is given by  $\omega_Z + \Omega_Q[\mathbf{r}_i(t), t]$  and depends on time ( $t$ ) via  $\mathbf{a}_i = \mathbf{a}_i[\mathbf{r}_i(t), t]$ , i.e., the instantaneous orientation of the molecular long axis.

Neglecting for a moment translational diffusion, the coordinates of a given molecule  $\mathbf{r}_i$  can be taken as fixed and time-independent during the NMR experiment. The long molecular axis  $\mathbf{a}_i$ , however, still fluctuates around the local average, i.e., the director  $\mathbf{n}(\mathbf{r}_i)$ , and thus still depends on  $t$ . Hence, we have  $\mathbf{a}_i = \mathbf{a}_i(\mathbf{r}_i, t)$  and, consequently,  $\Omega_Q = \Omega_Q(\mathbf{r}_i, t)$ : the time dependence in  $\Omega_Q$  is caused by the fluctuations of  $\mathbf{a}_i$  only, while the average  $\mathbf{a}_i$  remains fixed. Further, we have assumed a secular spin Hamiltonian that excludes spin flips as the orientation varies. To simulate such a dynamics we calculate spectra using the data from 1024 successive Monte Carlo simulation steps. The characteristic time scale for orientational fluctuations  $t_F$  in a typical liquid crystal is of the order of  $\sim 10^{-8}$  s [21]. The dynamics of Monte Carlo simulations is determined by the arbitrary molecular evolution process chosen (in contrast to molecular dynamics simulations), and hence the time scale assigned to fluctuations generated by this technique does not necessarily have to match with the natural time scale indicated above. However, the update process we have adopted here moves one molecule at a time for a certain angular step and is thus a plausible physical evolution process. In this sense, we can map the MC dynamics onto a plausible real one apart from an arbitrary time unit.

Including now the translational diffusion as well, molecular coordinates change during the NMR experiment, i.e.,  $\mathbf{r}_i = \mathbf{r}_i(t)$ . Thereby the average  $\mathbf{a}_i$  for a given molecule changes with time since  $\mathbf{n} = \mathbf{n}(\mathbf{r}_i)$ , and therefore the instantaneous  $\mathbf{a}_i$  depends on  $t$  also indirectly through  $\mathbf{r}_i = \mathbf{r}_i(t)$ . In this case we can now write  $\mathbf{a}_i = \mathbf{a}_i[\mathbf{r}_i(t), t]$  and  $\Omega_Q = \Omega_Q[\mathbf{r}_i(t), t]$ . The typical time scale for a diffusion yielding a displacement for one molecular length ( $\sim 1$  nm),  $t_D$ , is, like  $t_F$ , also of the order of  $\sim 10^{-8}$  s [21]. It is, however, more relevant to know the time  $t'_D$  needed for a molecular diffusion to yield a displacement over which the average molecular orientation [i.e., the director field  $\mathbf{n}(\mathbf{r})$ ] changes considerably. This distance obviously varies with the system size, i.e., the droplet radius  $R$ , so the relevant diffusion time  $t'_D$  can become much larger

than  $t_D$ . In other words, in smaller droplets effects of translational diffusion can be much more important than in larger ones.

In order to estimate how dynamic processes influence the spectra, it is necessary to compare their characteristic time scales to the characteristic NMR time scale  $t_0 \approx 2\pi/\delta\omega_Q$ , which, for the deuterium quadrupolar splitting in the nematic phase, is of the order of  $\sim 10^{-5}$  s. If the molecular motion is sufficiently slow on the NMR time scale  $t_0$ , the spectra can be calculated as  $I(\omega) = \langle \delta[\omega - \omega_Z \pm |\omega_Q(\mathbf{r}_i)|] \rangle_i$  [2], i.e., it is possible to use the static approach used in Refs. [6,14]. If, at the other extreme, the motion is very fast on the  $t_0$  scale, the spectrum is completely motionally averaged and now consists of a sharp doublet  $I(\omega) = \delta[\omega - \omega_Z \pm \langle |\omega_Q(\mathbf{r}_i)| \rangle_i]$  whose peaks are positioned at average frequencies  $\pm \langle |\omega_Q(\mathbf{r}_i)| \rangle_i$  [2].

Here we would like to calculate systematically the NMR spectra for different director configurations in nematic droplets, proceeding from the static limit to the limit of completely motionally averaged spectra, in order to find out to which extent diffusive processes smear the spectra and thus make the identification of director configurations impossible. To see this effect, a number of simplifying assumptions, described later, has to be invoked. Note also that in Eq. (1) we have assumed no coupling between the spectrometer magnetic field  $\mathbf{B}$  and the molecular orientation. Indeed, in microconfined liquid crystals the aligning effects of a magnetic field can be ignored if the magnetic coherence length  $\xi \propto 1/B$  [22] is much larger than the characteristic dimension of the confined system, i.e., if the magnetic field is weak enough that it cannot overwhelm the aligning effects of the confining walls. In our case, the condition  $\xi \gg R$  ( $R$  denoting the droplet radius) must be fulfilled to justify omitting the molecular coupling with the spectrometer field.

## IV. RESULTS

### A. Molecular fluctuations

Let us first consider spectra in absence of translational diffusion, or, equivalently, spectra of large enough nematic droplets (with  $R \gg \sqrt{6Dt_0}$ ) in which this kind of molecular motion can be considered as rather unimportant. The only relevant molecular dynamics is now caused by fluctuations of long molecular axes  $\mathbf{a}$  around the director  $\mathbf{n}$ . In order to obtain a spectrum with a sufficient resolution, it is necessary to simulate a relaxation signal  $G(t)$  that is long enough, i.e., lasting for several NMR cycles of duration  $t_0$  each. Comparing the time scales of molecular fluctuations and NMR, i.e.,  $t_F$  and  $t_0$ , it is evident that there should be about  $10^3$  molecular fluctuations per NMR cycle. This relation between  $t_0$  and  $t_F$  does not allow us to generate a sufficiently long  $G(t)$ , as, for technical reasons, we only have the data for 1024 successive MC spin configurations available. Therefore, generating  $G(t)$  we decided to update the spin configuration from the MC data less frequently than required by the natural time scale  $t_F$  in order to cover a long enough period in time. This approximation is not of essential importance given the already mentioned arbitrariness in the Monte Carlo time scale.

In the case without diffusion we decided to update spin configurations inside the nematic droplet eight times per

NMR cycle, this being much less than the natural scale given above. This enabled us then to generate a  $G(t)$  signal whose length is  $128 t_0$ , yielding spectra with a resolution of 256 points in the relevant (nonzero) part of the spectrum. It is possible to check whether this frequency of configuration sampling is sufficient or not by comparing the order parameter  $S$  deduced from the NMR spectra and from the MC data themselves. Further, the resulting spectra show some ‘‘noise’’ because the number of spins inside the droplet is still relatively small. To smoothen these spectra, a convolution with a Gaussian kernel of width  $0.04\delta\omega_Q$  has been performed. For  $\delta\omega_Q \sim 2\pi \times 100$  kHz this width equals  $\sim 2\pi \times 4000$  Hz, which is well above the natural line width, typically given by  $\sim 2\pi \times 100$  Hz. Note that neither the width of the kernel nor its shape (Gaussian instead of Lorentzian) match with the features of natural single-spin NMR lines and that the purpose of performing such a convolution was merely to smoothen the spectra and not to simulate the natural linewidth.

In the following we are going to consider nematic droplets with three different types of boundary conditions: radial (RBC), bipolar (BBC), and random (RND). The RBC are obtained when the spins in the outermost layer of the sample representing the polymer matrix (ghost spins) are oriented normal to the local surface. In case of BBC the ghost spins are fixed tangentially to this surface and in planes containing the  $z$  axis. Finally, random boundary conditions are simulated by a random orientational distribution of the ghost spins. In all cases the orientation of these spins remains fixed during the simulation.

According to Eq. (2), the full width of a doublet in the spectrum equals  $2\delta\omega_Q S$ . In the perfectly aligned nematic phase with  $S=1$  the spectrum width amounts to  $2\delta\omega_Q$ , but as soon as dynamic effects are taken into account, the spectrum is narrowed, and molecular fluctuations effectively yield  $S < 1$ . The spectrum of, e.g., the RBC droplet, in which molecular orientations are distributed isotropically over the whole solid angle, is equivalent to the Pake-type powder spectrum [19] consisting of two asymmetric peaks positioned at  $\omega_Z \pm \frac{1}{2}\omega_Q S$  (see the top curve in Fig. 1). Therefore, it is possible to deduce the value of  $S$  from the actual position of these peaks: in our case  $S \approx 0.72 \pm 0.02$ . To check this result we have calculated  $S$  also directly from the MC data by diagonalizing the time averaged ordering matrix for each of the spins and averaging the largest eigenvalues obtained in this way over the whole droplet. Such a calculation gives  $S \approx 0.73$ . This rather good agreement also indicates that even sampling MC structures rather infrequently (i.e., only eight times per NMR cycle) in order to generate a longer  $G(t)$  still reproduces the effect of molecular fluctuations sufficiently well.

The spectrum of the BBC droplet in the no-diffusion limit differs considerably from that of the RBC droplet. If the NMR magnetic field  $\mathbf{B}$  is applied along the  $z$  axis (i.e., the symmetry axis of the droplet), it still has two asymmetric peaks, which, however, are now located at  $\omega_Z \pm \omega_Q S$ . This reveals that indeed most of the molecules are aligned parallel to  $\mathbf{B}$  (see the top curve in Fig. 2). Evaluating  $S$  from the peak positions  $S \approx 0.74 \pm 0.02$  is obtained, while calculating  $S$  directly from the MC data yields  $S \approx 0.76$ . Again the agreement of the two estimates is good. In general, bipolar sym-

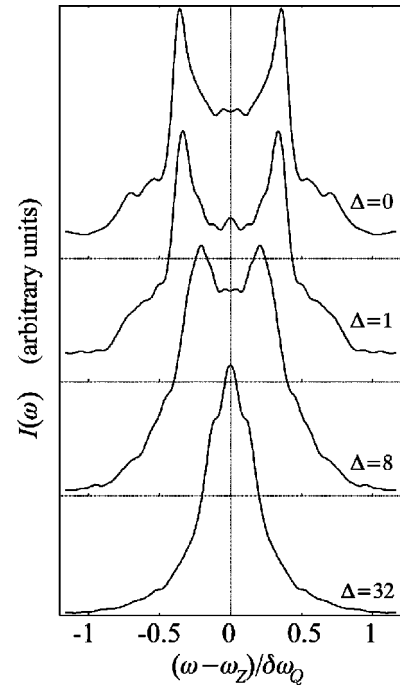


FIG. 1.  $^2\text{H}$  NMR spectra of the radial droplet for different values of the diffusion parameter  $\Delta$ :  $\Delta=0$  corresponds to the no-diffusion limit, while  $\Delta=32$  corresponds to the fast diffusion limit. The Pake-type powder spectrum obtained for  $\Delta=0$  collapses into a single line centered at zero quadrupolar splitting for  $\Delta=32$ . All spectra have been normalized so as to obtain the same peak height.

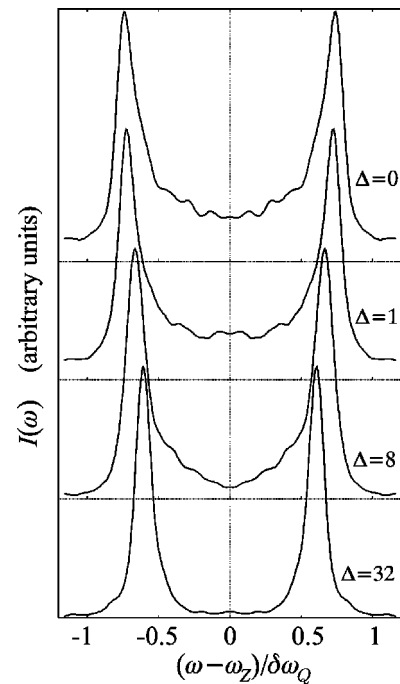


FIG. 2.  $^2\text{H}$  NMR spectra of the bipolar droplet for different values of  $\Delta$ . The spectrometer magnetic field is aligned along the bipolar symmetry axis, which results in a spectrum consisting of two lines both in absence of diffusion ( $\Delta=0$ ) and in the fast diffusion limit ( $\Delta=32$ ).

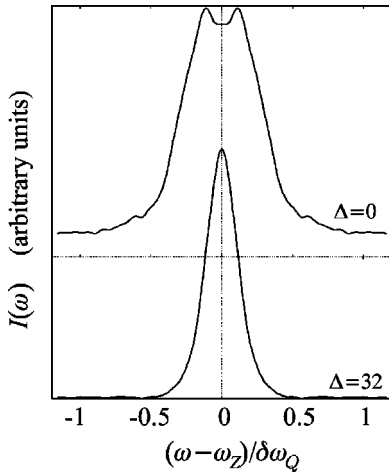


FIG. 3.  $^2\text{H}$  NMR spectra of the droplet with random boundary conditions and with the spectrometer field directed along the  $z$  axis. The molecular alignment at the “magic” angle with respect to  $z$  gives rise to a very small ( $\Delta=0$ ), or even zero splitting ( $\Delta=32$ ).

metry axes in droplets of a PDLC sample can have arbitrary spatial orientations. Summing up contributions originating from droplets all over the sample then yields a spectrum similar to the Pake-type powder spectrum [15]. If, however, the process of nematic droplet formation in a polymer matrix is occurring in a sufficiently strong external magnetic field, the bipolar droplet axes align along the field direction. This frozen-in alignment can be retained also after the field has been switched off [2], which then corresponds to the case considered here. We further assume the magnetic field of the NMR spectrometer to be directed along the droplet axes.

The spectrum of the nematic confined to a droplet with random boundary conditions does not show any sharp peaks when, again, the spectrometer field  $\mathbf{B}$  is applied along  $\mathbf{z}$ , i.e., the  $z$  axis (Fig. 3, top curve). There are just two broad peaks centered at  $\sim \omega_z \pm 0.1 \delta \omega_Q$ . The direct calculation of  $S$  from MC data yields  $0.67$ , which indicates that by coincidence the angle between  $\mathbf{B}$  and the director in a large part of the droplet must be close to the “magic” angle giving rise to zero (or at least very small) quadrupolar splitting. Rotating the sample with respect to  $\mathbf{B}$  and calculating the corresponding spectra indeed reveals the existence of some net molecular alignment in the droplet core. This ordered structure is due to the fact that the ordering effect of the Lebwohl-Lasher potential overcomes the disordering effect induced by the random boundary conditions at the droplet surface. However, the direction of alignment in the ordered core is arbitrary and depends on the random orientations at the border surface and on the starting configuration. During the Monte Carlo evolution the core can change its alignment, although this reorientation should be very slow at the low temperatures at which we have performed our simulations. For all these reasons, note that the spectra given in Fig. 3 are not unique. Namely, choosing, e.g., a different MC starting configuration could result in quite a different spectrum, not necessarily consisting of a single line like the spectra shown in Fig. 3.

The existence of this ordered core is confirmed also by calculating the average nematic director  $\langle \mathbf{n} \rangle$  directly from the MC data. In the  $xyz$  reference frame it is given by  $\langle \mathbf{n} \rangle \approx (0.205, 0.722, 0.660)$ . Setting  $\mathbf{B} \parallel \langle \mathbf{n} \rangle$ , the spectrum shows

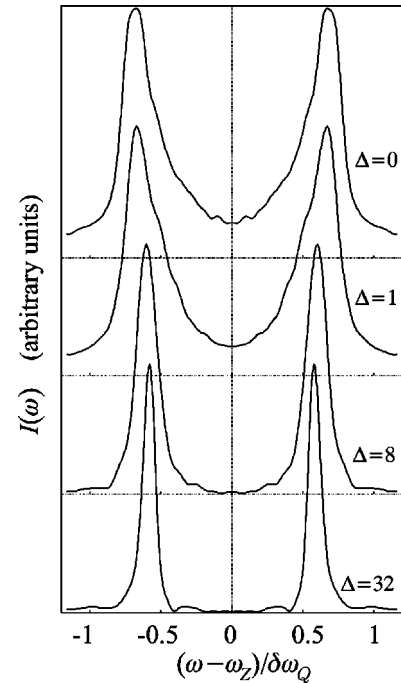


FIG. 4.  $^2\text{H}$  NMR spectra of the droplet with random boundary conditions and with the spectrometer field directed along the average director  $\langle \mathbf{n} \rangle$  calculated from the MC data. The two peaks in the spectrum occur at nonzero splitting both for  $\Delta=0$  and for  $\Delta=32$ .

two lines (Fig. 4, top curve), positioned approximately at the maximum splitting  $\sim \delta \omega_Q S$ . Deducing the value of  $S$  from the position of these two lines now yields  $0.67 \pm 0.02$ , which is again in a very good agreement with the MC data. Since in a droplet with random boundary conditions a substrate-induced net easy axis does not exist, the average molecular direction  $\langle \mathbf{n} \rangle$  in the core of the droplet will be completely arbitrary. In our simulation the droplet is already large enough (5832 spins) to allow the presence of an ordered nematic core in the bulk, while closer to the droplet wall the degree of ordering is lower, due to the disordering effect of the confining substrate. Performing the same type of simulations for a droplet of smaller size (1476 spins) still shows similar core ordering effects which, however, are somewhat weaker since now the fraction of molecules disordered by the surface is higher than in the previous case.

### B. Translational diffusion

In addition to fluctuations of the long molecular axes we would now like to include also translational molecular diffusion into the analysis. Let us consider, for simplicity, the case in which the diffusion is characterized by a single motional constant (the diffusion tensor is isotropic), i.e., the probability for a molecular diffusion does not depend on the local orientation of the director. In a bulk unconstrained nematic phase the diffusion anisotropy can be typically up to  $D_{\parallel}/D_{\perp} \approx 2$ , with  $D_{\parallel}$  being measured along the director and  $D_{\perp}$  perpendicular to it [2,22]. Our tests indicate, however, that the inclusion of anisotropic diffusive processes into the simulation alters the spectra only negligibly.

Translational diffusion has been simulated by a simple random process in which the spins representing one or more nematic molecules jump between lattice sites. In each simu-

lation step each of the spins is allowed to move to its nearest neighbor site with equal probability in the present isotropic case, while in the anisotropic case this probability has to be biased so as to increase the diffusion probability along the director [2]. After the diffusion jump has been performed, the spin acquires a new orientation, whose average (i.e., the local director) in a distorted sample is different from the average calculated at the old coordinates. Calculating  $G(t)$  we have, like in the diffusionless case, updated the spin configuration inside the droplet from the MC data eight times per NMR cycle. Now additional diffusion steps have been added in between these structural updates, with their number  $\Delta$  ranging from 1 to 32. In this last case the spectra are completely motionally averaged due to diffusion effects, since for  $\Delta=32$  each of the spins exhibits a total of 256 jumps within the duration of one NMR cycle, this already corresponding to the fast diffusion limit with  $t'_D \ll t_0$ .

We start by considering the case of radial boundary conditions. Figure 1 shows a sequence of RBC droplet spectra, ranging from the no-diffusion limit ( $\Delta=0$ ) to the fast diffusion limit ( $\Delta=32$ ). In general, for any type of boundary conditions the fast diffusion spectrum consists of two lines centered at  $\omega_Z \pm \langle \omega_Q \rangle_i$ , where the average frequency is given by  $\langle \omega_Q \rangle_i = \delta\omega_Q S \langle \frac{1}{2} [3 \cos^2 \theta(\mathbf{r}_i) - 1] \rangle$ . If the diffusion is fast enough so that molecules diffuse through a large enough portion of the droplet, in the radial configuration where  $\langle \omega_Q \rangle_i = 0$  holds, the two lines should coalesce into a central line (zero quadrupolar splitting). Inspecting the simulated spectra (the sequence in Fig. 1), it is evident that this indeed happens. It is possible to deduce the value of  $\langle \omega_Q \rangle_i$  also directly from the MC data, yielding  $\langle \omega_Q \rangle_i \approx 0.03 \delta\omega_Q$ .

Repeating the same analysis for the bipolar droplet, we observe that the two lines in the spectrum do not merge into a single line as we have just observed for the radial droplet when moving from the slow into the fast diffusion regime (Fig. 2). This happens because now we are dealing with an ensemble of molecules whose orientational distribution is spatially anisotropic. Hence,  $\langle \omega_Q \rangle_i \neq 0$  should be expected, unless (by coincidence) the relative orientation between the NMR spectrometer magnetic field and the majority of spins within the droplet yields  $\omega_Q \sim 0$  already in itself. This is, however, not the case for the spectra shown in Fig. 2: here  $\langle \omega_Q \rangle_i = (0.61 \pm 0.02) \delta\omega_Q$  from the peak positions and  $0.59 \delta\omega_Q$  from the MC data. On the contrary,  $\omega_Q \sim 0$  happens when considering the droplet with random boundary conditions if the NMR magnetic field is applied along  $\mathbf{z}$ . As a consequence, the spectrum is then averaged into a single line centered at  $\langle \omega_Q \rangle_i = 0$  (see Fig. 3, bottom curve) although there is net molecular alignment in the droplet core, as already pointed out in the previous subsection (MC data here yield  $\langle \omega_Q \rangle_i \approx 0.09 \delta\omega_Q$ ). Also in the fast diffusion limit this alignment can be explored by imposing a spectrometer magnetic field  $\mathbf{B}$  oriented along directions other than the  $z$  axis (e.g., along  $x$  and  $y$  axes, or along  $\langle \mathbf{n} \rangle$ ), resulting in spectra that consist of two lines (for  $\mathbf{B} \parallel \langle \mathbf{n} \rangle$  see Fig. 4). The agreement of the line positions and the MC data is still rather good: for  $\mathbf{B} \parallel \mathbf{x}$   $\langle \omega_Q \rangle_i \approx (0.24 \pm 0.02) \delta\omega_Q$  (peak position) versus  $\langle \omega_Q \rangle_i \approx 0.25 \delta\omega_Q$  (MC data), for  $\mathbf{B} \parallel \mathbf{y}$   $\langle \omega_Q \rangle_i \approx (0.175 \pm 0.02) \delta\omega_Q$  (peak) versus  $\sim 0.16 \delta\omega_Q$  (MC), and, finally, for

$\mathbf{B} \parallel \langle \mathbf{n} \rangle$   $\langle \omega_Q \rangle_i \approx (0.58 \pm 0.02) \delta\omega_Q$  (peak) versus  $\sim 0.59 \delta\omega_Q$  (MC).

As indicated before, diffusive processes are expected to be more important in small droplets than in large ones. Therefore, it is convenient to express the limit between the slow and fast diffusion regimes in terms of the droplet size, keeping the value of the diffusion constant fixed (e.g., to  $D \approx 10^{-10}$  m<sup>2</sup>/s). This can be done since the spins used for modeling the nematic can be interpreted also as close packed clusters of several (up to  $\sim 100$ ) molecules [6]. Putting the droplet radius  $R$  as an estimate for the characteristic length over which  $\mathbf{n}(\mathbf{r})$  changes considerably and  $t'_D \approx t_0 \approx 10^{-5}$  s give  $R = \sqrt{6Dt_0} \approx 75$  nm. Hence, for these particular values of  $D$  and  $t_0$  in droplets with  $R \gg 75$  nm diffusive effects can be neglected while in those with  $R \lesssim 75$  nm this cannot be done.

Lining up spectra for the three different types of boundary conditions and comparing them shows that in the slow diffusion limit it is always possible to identify the radial structure because of its characteristic Pake-type form of the spectrum, which does not depend on the direction of the spectrometer magnetic field. The spectra of the bipolar and the random droplets, on the other hand, depend significantly on the magnetic field direction since the corresponding director configurations are anisotropic due to the bulk net molecular alignment. Consequently, the spectra of the two droplets are similar and difficult to distinguish. All these conclusions hold also in the fast diffusion regime, except that the Pake-type spectrum of the radial droplet collapses into a single line at zero splitting, again regardless of the magnetic field direction. The diffusion-averaged spectra of the other two structures show two peaks at nonzero splitting, unless, again, the majority of the spins is lying at a ‘‘magic’’ angle with respect to the spectrometer field direction.

## V. CONCLUSION

In the present analysis we have calculated <sup>2</sup>H NMR spectra of polymer-dispersed liquid crystals (PDLC) in order to investigate orientational molecular ordering and dynamics within nematic droplets. The input data for the calculation of the NMR spectra were provided from Monte Carlo simulations, where the nematic droplet was modeled using the Lebwohl-Lasher lattice model. In this approach dynamic effects such as fluctuations of molecular long axes and effects of translational diffusion can easily be included. Therefore, we could focus on establishing a relation between the dynamical processes within nematic droplets and the resulting NMR spectra. The polymer matrix confining the droplets was chosen to impose three different types of boundary conditions: radial, bipolar, and random, which can be encountered also in a real experimental setup.

Our results indicate that, as predicted, molecular fluctuations lead to a narrowing of the NMR spectrum, while its shape remains similar to that obtained in the static case. From this narrowing it is possible to deduce the value of  $S$ , the order parameter, which turns out to be in an excellent agreement with the value deduced directly from the Monte Carlo data. Further, molecular diffusive motions result in an averaged spectrum, which in the fast diffusion limit consists of one or two rather narrow lines, depending on the type of

boundary conditions. Once the direction of the NMR magnetic field has been fixed, it is also possible to predict the position of these lines from the Monte Carlo data, and again the agreement with the actual spectra is fairly good.

Moreover, the shape of NMR spectra depends on the type of the boundary conditions considered, and, in general, on the relative orientation of the NMR magnetic field and the director structure occurring in the droplet. According to our results it is always possible to recognize the signature of the radial droplet, while it is almost impossible to distinguish between those of the bipolar and random ones. In fact, the NMR spectra reveal net molecular alignment also in the core of the random droplet, and hence the director field is roughly

similar to that in the bipolar one, which, in turn, results in similar NMR spectra.

#### ACKNOWLEDGMENTS

C.Z. wishes to thank the University of Bologna, CNR, and MURST for support. C.C. and P.P. are grateful to the INFN for support through Grant No. IS BO12. G.S. and S.Ž. wish to acknowledge the financial support of the Ministry of Science and Technology of Slovenia (Grant No. J1-0595-1554-98) and of the European Union (Project INCO Copernicus No. ERBIC15CT960744).

- 
- [1] G. P. Crawford and S. Žumer, *Liquid Crystals in Complex Geometries Formed by Polymer and Porous Networks* (Taylor and Francis, London, 1996).
- [2] A. Golemme, S. Žumer, J. W. Doane, and M. E. Neubert, *Phys. Rev. A* **37**, 559 (1988).
- [3] R. Ondris-Crawford, E. P. Boyko, B. G. Wagner, J. H. Erdmann, S. Žumer, and J. W. Doane, *J. Appl. Phys.* **69**, 6380 (1991).
- [4] P. Drzaic, *Mol. Cryst. Liq. Cryst.* **154**, 289 (1988).
- [5] R. Aloe, G. Chidichimo, and A. Golemme, *Mol. Cryst. Liq. Cryst.* **203**, 9 (1991).
- [6] C. Chiccoli, P. Pasini, F. Semeria, E. Berggren, and C. Zannoni, *Mol. Cryst. Liq. Cryst.* **266**, 241 (1995).
- [7] P. A. Lebowitz and G. Lasher, *Phys. Rev. A* **6**, 426 (1972).
- [8] U. Fabbri and C. Zannoni, *Mol. Phys.* **58**, 763 (1986).
- [9] C. Chiccoli, P. Pasini, F. Semeria, and C. Zannoni, *Phys. Lett. A* **150**, 311 (1990); *Mol. Cryst. Liq. Cryst.* **212**, 197 (1992).
- [10] C. Chiccoli, P. Pasini, F. Semeria, and C. Zannoni, *Mol. Cryst. Liq. Cryst.* **221**, 19 (1992).
- [11] E. Berggren, C. Zannoni, C. Chiccoli, P. Pasini, and F. Semeria, *Chem. Phys. Lett.* **197**, 224 (1992).
- [12] N. Metropolis, A. W. Rosenbluth, M. N. Rosenbluth, A. H. Teller, and E. Teller, *J. Chem. Phys.* **21**, 1087 (1953).
- [13] J. A. Barker and R. O. Watts, *Chem. Phys. Lett.* **3**, 144 (1969).
- [14] E. Berggren, C. Zannoni, C. Chiccoli, P. Pasini, and F. Semeria, *Phys. Rev. E* **49**, 614 (1994).
- [15] A. Golemme, S. Žumer, D. W. Allender, and J. W. Doane, *Phys. Rev. Lett.* **61**, 2937 (1988).
- [16] M. Ambrožič, P. Formoso, A. Golemme, and S. Žumer, *Phys. Rev. E* **56**, 1825 (1997).
- [17] J. Dolinšek, O. Jarh, M. Vilfan, S. Žumer, R. Blinc, J. W. Doane, and G. Crawford, *J. Chem. Phys.* **95**, 2154 (1991).
- [18] R. Y. Dong, *Nuclear Magnetic Resonance of Liquid Crystals* (Springer-Verlag, New York, 1994).
- [19] A. Abragam, *The Principles of Nuclear Magnetism* (Clarendon Press, Oxford, 1961).
- [20] C. Zannoni, in *The Molecular Physics of Liquid Crystals*, edited by G. R. Luckhurst and G. W. Gray (Academic, London, 1979), Chap. 9.
- [21] S. Žumer, P. Zihlerl, and M. Vilfan, *Mol. Cryst. Liq. Cryst.* **292**, 39 (1997).
- [22] P. G. de Gennes and J. Prost, *The Physics of Liquid Crystals* (Clarendon Press, Oxford, 1993).